BALKAN JOURNAL OF ELECTRICAL & COMPUTER ENGINEERING, Vol. 11, No. 3, July 2023

A Detailed Comparison of Two Different Switched Reluctance Motor's Parameters and Dynamic Behaviors by applying PID Control in Matlab Simulink

Bekir Gecer, N.Fusun Serteller and Huseyin Calik

Abstract—**The Switched Reluctance Motor (SRM) is one of the oldest types of electric motors. SRMs have high torque fluctuations as they have a salient pole structure. The popularity of Switched Reluctance Motors has increased in recent years due to their simple structure, ruggedness, reliability, as well as being inexpensive to manufacture and having a high torque to mass ratio. However, there are some disadvantages, such as high torque ripple, noise and the need for an advanced control system. So they are not extensively used in industry. This study focused on the torque ripple and the speed control aspects. Here, the two most popular and similar Switched Reluctance Motors with regard to motor size, called the 6/4 and 8/6 SRM, have been compared according to the dynamic behavior of their motor parameters. Also, the converters, loads and given power values are the same for the two motor systems. The motor parameters were controlled via MatLab Simulink software. Although the 6/4 and 8/6 models are identical and have the same power converters systems and position sensors, they show different motor behavior due to their dissimilar magnetic structures.**

Index Terms—**Switched Reluctance Motor, Simulink, PID Control.**

BEKIR GECER, is with Machine and Metal Technology Department of Atasehir Adiguzel Myo, Istanbul, Turkey,(e-mail: bekirgecer@adiguzel.edu.tr).

https://orcid.org/ 0000-0002-7803-3844

N.FUSUN SERTELLER, is with Electrical and Electronic Engineering Department of Marmara University, Istanbul, Turkey,(e-mail: fserteller@marmara.edu.tr).

https://orcid.org/ 0000-0003-3147-2740

HUSEYIN CALIK, is with Electrical and Electronic Engineering Department of Giresun University, Istanbul, Turkey,(e-mail: huseyin.calik@giresun.edu.tr).

https://orcid.org/ 0000-0001-8298-8945

Manuscript received Sep 19, 2022; accepted May 3, 2023.
DOI: 10.17694/bajece.1177168

I. INTRODUCTION

THE Switched Reluctance Motors (SRMs) are early members of the electric machine family. SRMs have high torque fluctuations as they have a salient pole structure. The popularity of Switched Reluctance Motors has increased in recent years due to their simple structure, ruggedness, reliability, and being inexpensive to manufacture and having a high torque to mass ratio. The SRM is a singly or doubly salient motor, and torque is produced by reluctance. Therefore, the rotor of the SRM has a tendency to move to a position of alignment where the inductance of the excited windings is maximized [1]–[4].Because of the advantages of SRMs and improvements in their motor control and drive systems, they are used in industrial and engineering applications. With the development of driver systems, more effective and efficient control strategies can be designed in order to increase the motor performance and system power efficiencies by decreasing the size and cost of the driver components. In conventional terms, the SRM has some disadvantages: it needs a position sensor and an advanced control system. It has a double salient structure that causes high torque ripple and noise. The torque ripple is the primary problem of SRMs in applications that require stable dynamic performance and low torque ripple [2], [5], [6]. The Ansys/Maxwell software program was also used in the study at reference [19] to understand SRM by analyzing. As well as SRM design studies; novel driver methods applications were worked for SRM [16]. An induction machine and a SRM have been compared for E-Scooter based driving cycle design in [17].

This study compared the almost identical 6/4 and 8/6 doubly salient reluctance motors according to the effect on dynamic behavior of their motor parameters I (Amps), V (Volts), Te (induced electromagnetic torque), ω (angular velocity), Φ (flux) and Θ (angle) used as control parameters by the MatLab Simulink software, respectively. See Fig 1 (a) and (b) illustrating the physical structures.

 ISSN: 2147-284X

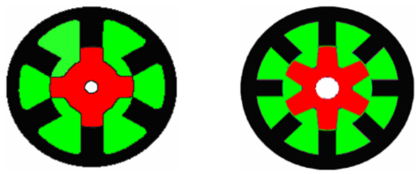

a) 6/4 Three Phase SRM b) 8/6 Four Phase SRM
Fig 1. SRM Configurations [8].

The alignment position of both motors is given in Fig 2(a). In a magnetic circuit, the rotating part wants to reach the position of minimum reluctance at the instance of excitation. The unaligned positions of both motors are shown in Fig 2(b). Then, the set of stator poles is excited to bring the rotor poles into alignment.

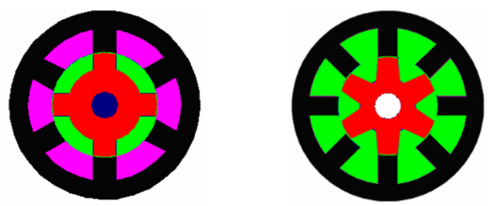

a) Aligned Position

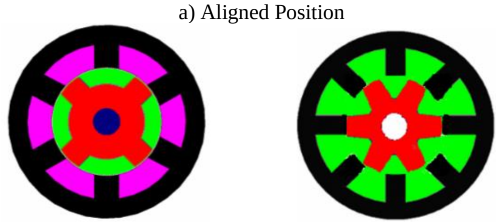

b) Unaligned Position
Fig 2. Operations of SRM [8].

II. DYNAMIC MODEL OF SRM

The dynamic model of SRM can be obtained as the following equations. These equations can obtain equivalent circuit seen in Fig 3.

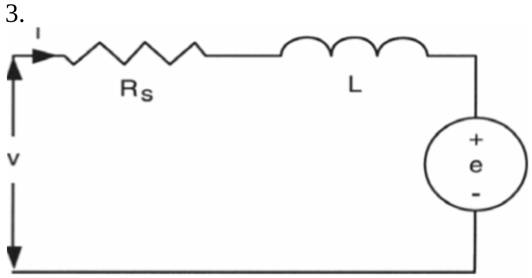

Fig 3. Single phase equivalent circuit of SRM.

The applied voltage to a phase is equal to the sum of the resistive voltage drop and the rate of the flux linkages and is given as Equation (1):

$$V = R_s i + \frac{d\lambda(\theta,i)}{dt} \tag{1}$$

where $R_s\ (\Omega)$ is the resistance per phase, i(A) is the phase current, θ(rad) is the rotor position and λ(Wb) the total flux linkage per phase given by:

$$\lambda = L(\theta,i)\, i \tag{2}$$

where L(H) is the inductance depended on the rotor position and phase current. Then, the phase voltage is derived:

$$V = R_s i + \frac{d(L(\theta,i)i)}{dt} = R_s i + L(\theta,i)\frac{di}{dt} + \frac{dL(\theta,i)}{d\theta} i\,\omega_m \tag{3}$$

Equation (3) consist of the three terms on te right-hand side: the resistive voltage drops, inductive voltage drop and induced emf, respectively. K_d is back-emf constant, $\omega_s\ (rad/s)$ is the angular speed of the rotor, the induced emf, e(V) can expressed briefly as:

$$e = \frac{dL(\theta,i)}{d\theta}\omega_m i = K_b\, \omega_m\, i \tag{4}$$

The electrical power is then:

$$V i = i^2 R + L(\theta,i) i \frac{di}{dt} + i^2 \omega_m \frac{dL(\theta,i)}{d\theta} \tag{5}$$

The mechanical power which is equivalent to where is the instantaneous electromagnetic torque [18].

$$T_e = \frac{1}{2} i^2 \frac{dL(\theta,i)}{d\theta} \tag{6}$$

The mechanical equation is:

$$J\frac{d\omega_m}{dt} = T_e + T_L - B\omega_m \tag{7}$$

where $J(kg.m^2)$ is inertia moment, B is friction coefficient.

TABLE 1. SRM Motor Parameters

SRM	6/4	8/6
Stator poles number	6	8
Rotor poles number	4	6
Stator resistant(ohm)	0.05	0.05
Friction coefficient (B.N.m.s)	0.02	0.005
Inertia J (kg.m^2)	0.05	0.01
Unaligned Inductance(H)	0.67e-3	0.67e-3
Aligned Inductance(H)	23.6e-3	23.6e-3
Voltage(V)	240	240
Current(A)	0-50	0-30

III. SIMULINK MODEL OF SRM WITH SPEED CONTROL TECHNIQUES

The Switched Reluctance Motor Control Simulink model has four main blocks. These are the controller block, the converter block, the position sensor block and the SRM blocks. The position sensor block is linked to the rotor of the Switched Reluctance Motor to measure the turn-on and turn-off angles of the Switched Reluctance Motor phases. These angles are necessary for switching the converter system. At the same time, the measured current and reference current are compared to generate drive signals for the converter systems. Then, the hysteresis controller controls the currents independently [21-24].

To analyze the performance of the SRM, the model of the entire drive system was developed in the position sensor mode in the simulation software Matlab/Simulink. The parameters for the voltage supply, V= 240 volts (DC) and the stator resistance, RS = 0.05 ohms/phase, were used for both the 6/4 and 8/6 SRM, respectively. The motor was loaded at TL =10 Nm between 0.1s to 0.2s, and raised by 20 Nm after 0.2 s and kept there until the end of the simulation. A SRM model is given in Fig 4 and the SRM Control Simulink Model of both motors is shown in Fig 5 and Fig 6. The motor parameters of both motors are seen Table 1. The PID controller values for 6/4 SRM are P=0.8, I=0.4 and D=0.03. Because of different poles number, 8/6 SRMs have different PID controller values are P=1.2, I=0.1 and D=0.01. If we change our reference speed, PID coefficient will be differ automatically. The PID gains of both SRMs are given in the Table 2.

TABLE 2. Controller PID Gains

PID GAIN	6/4	8/6
Proportional	0.8	1.2
Integral	0.4	0.1
Derivative	0.03	0.01

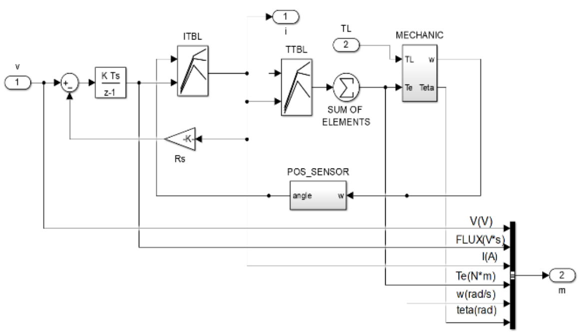

Fig 4. SRM Simulink Model.

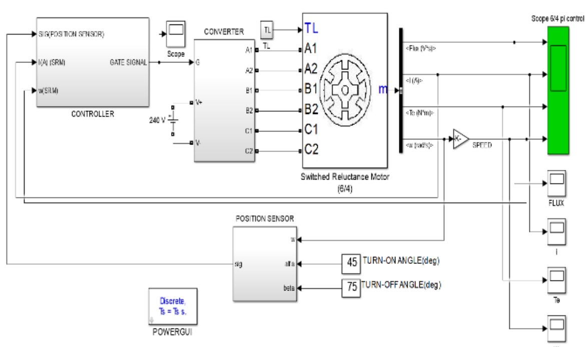

Fig 5. 6/4 SRM Control Simulink Model.

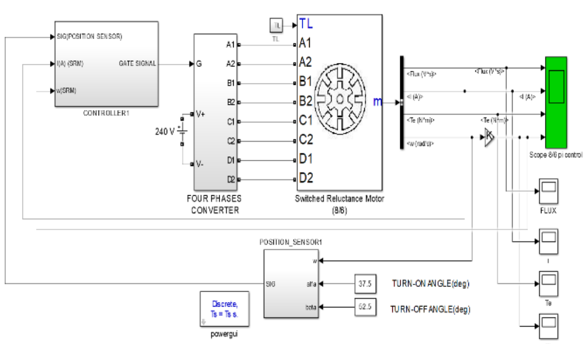

Fig 6. 8/6 SRM Control Simulink Model.

3. 1. Converter Topology

In this study, an asymmetric converter was used, which is the most usual and appropriate converter topology for the SRM. It is in the '2-switch per phase (2q switch)' converter group. The general structure of the asymmetric converter system is presented in Fig 7. Turning on the two power switches in each phase circulated a current in that phase of the SRM. If the current rose above the configd value, the switches were turned off. The energy stored in the motor phase winding keeps the current in the same direction until it is depleted [12, 19].

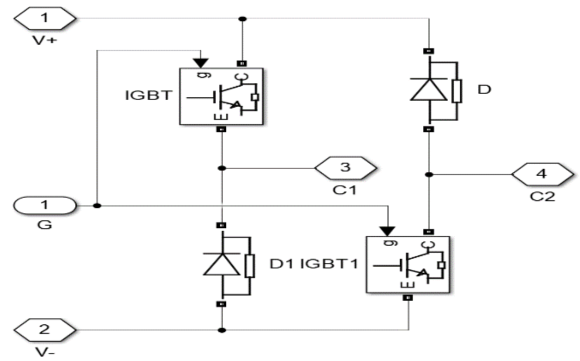

Fig 7. Converter Simulink Model for per phase.

3. 2. Controller Strategy

Fig 8 illustrates the Simulink diagram of the SRM controller that was used in simulations. It represents the Simulink diagrams for the SRM speed and position control. The position sensor value determines the command turn-on and turn-off, respectively, and generates the gate pulse for switching the SRM power converter. The gains of the PID controller, Kp, Ki and Kd, were adapted according to the rotor speed and they are adjustable. In the same way the SRM speed is controlled, the torque of the SRM is controlled by the feedback current. The 6/4 SRM shows more stable behavior than the 8/6 SRM in terms of speed control.

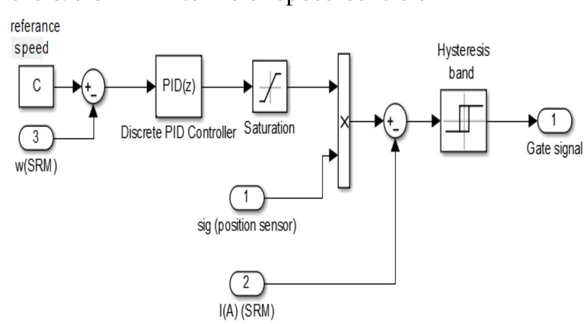

Fig 8. Controller Simulink Model.

3. 3. Position Sensor

In the SRM control systems, the rotor position is essential for the stator phase commutation and advanced angle control. The rotor position is acquired by the position sensors, which is shown in Fig 9. These blocks compare the rotor position with the reference turn-on and turn-off angle values to convert the output speed to the angle. For each motor, these reference angles can be changed due to the different motor structures. The position of both the 6/4 and 8/6 SRM was determined by taking the integral of the angular velocity and power supplied according to the turn-on and turn-off angles.

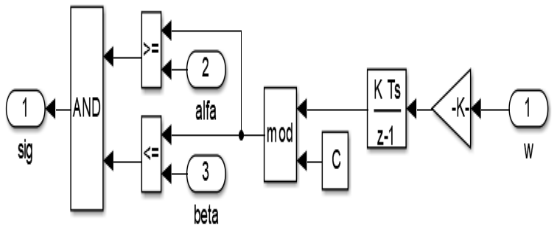

Fig 9. Position Sensor Simulink Model.

IV. Simulink Results and Discussion of SRM's Dynamic Behavior

Although 6/4 and 8/6 SRM models are almost identical, they show different motor performance due to their individual dynamic behavior. The motor parameters compared were I (A), the phase current, Te (Nm), the electromagnetic torque produced, ω (rad/s), the angular velocity of the rotor and Φ (Wb), the magnetic flux. As seen in Fig10, both the 6/4 and 8/6 SRMs are subject to a 10 Nm load between 0.11s and 0.20s. A second load of 20 Nm is applied after 0.20s. The behavior of the flux is seen in Fig 10. Because the flux depends on the current, the flux of the 6/4 SRM is greater than the flux of the 8/6 SRM, by about 0.5 Wb. When the load is being increased, the 6/4 SRM has higher flux values than the 8/6 SRM.

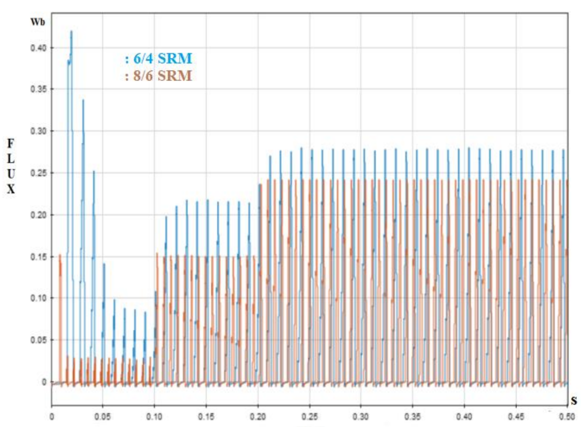

Fig 10. 6/4 and 8/6 SRM Flux Comparison.

When the loads are applied to the motors, changes in the motor currents are shown in Fig 11. It is seen that the 6/4 SRM draws 50% higher current than the 8/6 SRM. Because the 6/4 SRM's flux is higher than the 8/6 SRM.

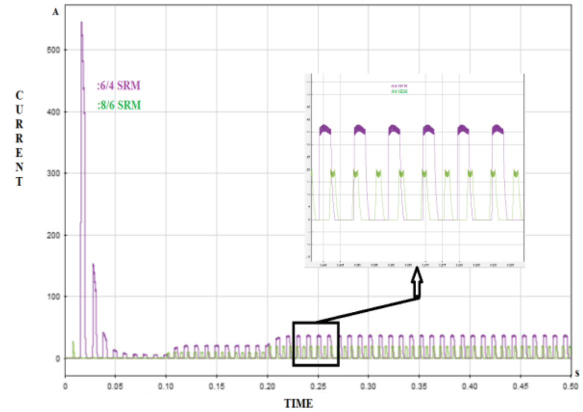

Fig 11. 6/4 and 8/6 SRM Current Comparison.

At a 10 Nm load the torque ripple 59.3% and at 20 Nm the torque ripple is 52%. At all load values, the 6/4 SRM current level was more than the 8/6 SRM current level due to the impact of its magnetic behavior.

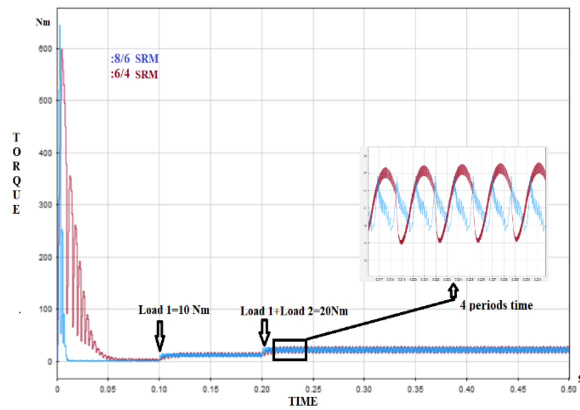

Fig 12. 6/4 and 8/6 SRM Torque Comparison.

Since the number of poles in the 8/6 SRM is more than the 6/4 SRM, the 8/6 torque ripple amplitude is less about 25% than the 6/4 torque ripple, as seen in Fig 12.

Under the loads conditions, the 8/6 SRM speed performance is higher than the 6/4 SRM and after 0.21 s the characteristics of the 8/6 SRM are more stable than the 6/4 SRM as seen in Fig 13.

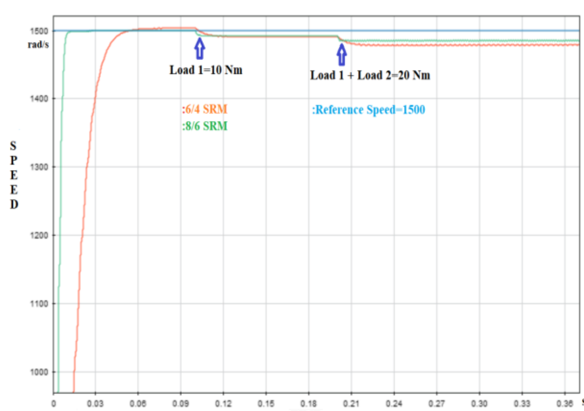

Fig 13. 6/4 and 8/6 SRM Speed Comparison.

Fig 14 shows the flux current variation of the 6/4 SRM. As can be seen from this fig, the continuous current value of the 6/4 SRM reaches 35 A. When the motor poles are in the centered position, the flux value is 0.025 Wb and when the motor poles are in the opposite position, it takes 0.27 Wb.

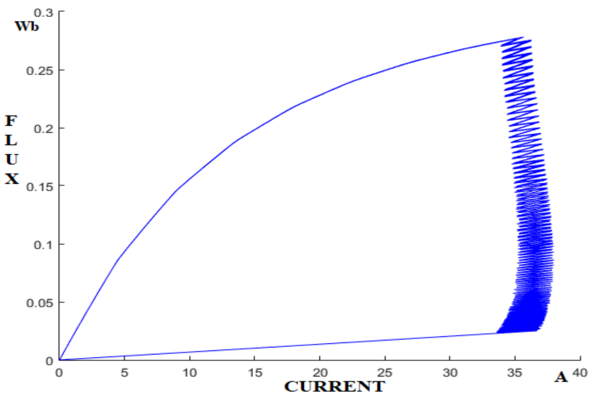

Fig 14. 6/4 SRM Flux-Current Behavior.

Fig 15 shows the flux current variation of the 8/6 SRM. As can be seen from the fig, the continuous current value of the 8/6 SRM motor reaches 18 A. The flux was 0.1 Wb when the motor poles were in the centered position and 0.24 Wb when the motor poles were in the opposite position.

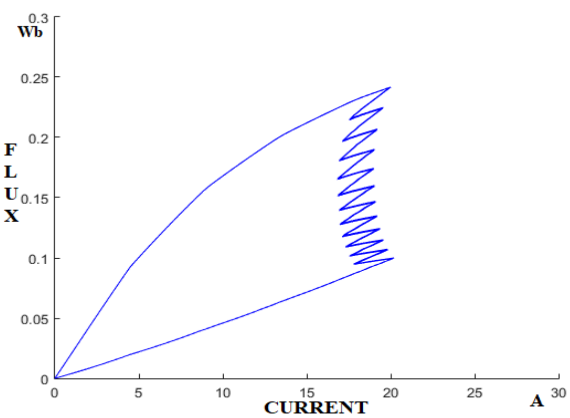

Fig 15. 8/6 SRM Flux-Current Behavior.

The 6/4 SRM characteristically draws more current than the 8/6 SRM, as shown in the current–flux graph. However, the 6/4 has higher flux Φ values, which causes more noise and vibration.

When the inductance graphs of the 6/4 SRM and the 8/6 SRM seen in Figs 16 and 17 were compared, we see that although they have same the minimum and maximum inductance values, their inductance frequencies due to the numbers of poles show different behaviors due to different current and flux values.

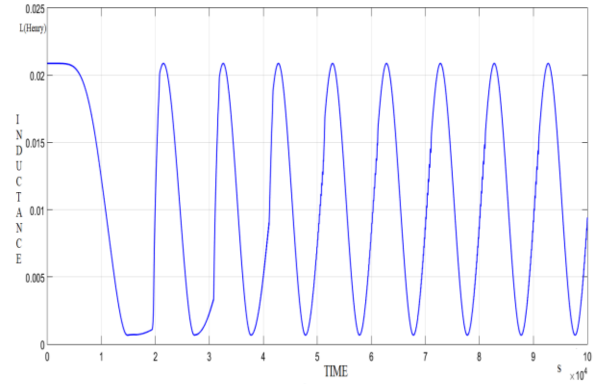

Fig 16. 6/4 SRM Inductance.

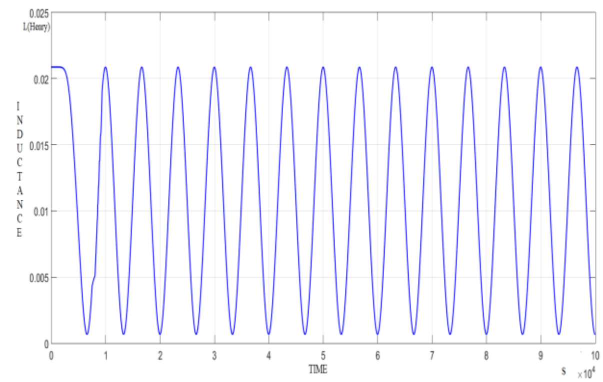

Fig 17. 8/6 SRM Inductance.

IV. CONCLUSION

This study illustrates the performance of two types of SRMs known as the 6/4 SRM and the 8/6 SRM. These motors are supplied by an asymmetric converter system and controlled by PID software. Although they are identical and have the same driver systems and position sensors, the motor performances are different due to their dissimilar magnetic structures. The simulation results show that 6/4 SRM carries more current than 8/6 SRM in the case of no load and loaded conditions, whereas 8/6 SRM has less 25 % torque ripple. Also, 6/4 SRM has 50% higher flux than 8/6 SRM due to the different poles number and unlike magnetic structure. Besides 6/4 SRM shows the better performance at low speeds.

REFERENCES

[1] Garlet, Tais B., Savian, Fernando S., Siluk, Julio C.M., (2019), "Research, development and innovation management in the energy sector", Advances in Energy Research, Volume 6, Issue 1, 17-33.

[2] Gujarathi, Pritam K., Shah, Varsha A., Lokhande, Makarand M., (2020), "Hybrid artificial bee colony-grey wolf algorithm for multi-objective engine optimization of converted plug-in hybrid electric vehicle", Advances in Energy Research, Volume 7, Issue 1, 35-52.

[3] Nematollahi, Amin Foroughi, Shiva, Navid, (2020), "An application of LAPO: Optimal design of a stand alone hybrid system consisting of WTG/PV/diesel generator/battery", Advances in Energy Research, Volume 7, Issue 1, 67-84.

[4] Kioskerides, I., Mademlis C., (2005), "Maximum efficiency in single-pulse controlled switched reluctance motor drives", IEEE Transactions on Energy Conversion, Volume 20, 809–817.

[5] Gorden R., Straughen A., (2000), "Electric machines", 1st Edition.

[6] Neuhaus, C., Fuengwarodsakul N. and Doncker R., (2006), "Predictive pwm-based direct instantaneous torque control of switched reluctance drives", Power Electronics Specialists Conference, 1–7.

[7] Krishnan, R., (2001), “Switched reluctance motor drives modelling”, CRC Press, London.
[8] Aljaism, W., (2015), “Switched reluctance motor design simulation and control”, University of Western Sydney School of Engineering DRG Power Conversion and Intelligent Motion Control.
[9] Vikramarajan, J., (2016), “Matlab simulink implementation of switched reluctance motor with direct torque control technique”, Volume 4, ISSN 2321–9939.
[10] Hashem, G., Hasanien H., (2010) “Speed control of switched reluctance motor based on fuzzy logic controller”, Proceedings of the 14th International Middle East Power Systems Conference (MEPCON’10).
[11] Wichert T., Staszewski P., (2008), “Design and construction modifications of switched reluctance machines”, Warsaw University of Technology Ph.D. Thesis.
[12] Farah N., Jurifa L., (2017), “Multilevel inverter fed switched reluctance motors (srms) 6/4, 8/6 and 10/8 srm geometric types”, International Journal of Power Electronics and Drive System (IJPEDS), Volume 8, ISSN 2088–8694.
[13] Toker K., Serteller F.N., (2017), “A dynamic analysis of bldc motor by using matlab/simulink and mathematica”, Conference on Electrical Electronics Engineering (CHILECON).
[14] Kentli F, Çalik H., (2011), “Matlab-Simulink modelling of 6/4 srm with static data produced using finite element method”, Acta Polytechnica Hungarica, 23–46.
[15] Nutan S., Panda S., (2017), “Speed control with torque ripple reduction of switched reluctance motor by many optimizing liaison technique”, Journel of Electrical Systems and Information Technology (JESIT).
[16] Grace L., Nguyen X., (2020), “Design of a low torque ripple three-phase srm for automotive shift-by-wire actuator”, Energies.
[17] Honzhong M., Chaozhi H., (2020), “The effect of a single-sided pole shoe and slot on reducing torque ripple in a switched reluctance motor”, Concurrency and Computation: Practice and Experience.
[18] Gecer B., Serteller F., (2019), “Investigation of effect of pole number change on operation parameters in switched reluctance motors”, Marmara University Electrical and Electronic Engineering.
[19] Sun H., Moghaddam A., (2020), “A novel driving method for switched reluctance motor will standard full bridge inverter, IEEE Transactions on Energy Conversion.
[20] Tuan V., Kreuawan S., (2020), “Switched reluctance motor and induction machine for e-scooter based on driving cycles design comparasion”, Transactions on Electrical and Electronic Engineering.
[21] Howey B., Liang J., (2020), “Making the case for switched reluctance motors for propulsion applications”, IEEE Transactions on Vehicular Technology.
[22] Gecer B., Serteller F., (2020), “Understanding switched reluctance motor analysis using ansys/maxwell”. IEEE 29th International Symposium on Industrial Electronics (ISIE).
[23] Gecer B., Tosun O., Apaydin H., Serteller F., (2021), “Comparative Analysis of SRM, BLDC and Induction Motor using ANSYS/Maxwell ”, Electrical, Computer, Communications and Mechatronics Engineering (ICECCME), International Conference.
[24] Gecer B., Serteller F., (2020), “Understanding a switched reluctance motor control and analysis methods using Matlab/simulink”. IEEE World Engineering Education Conference (EDUNINE).

BIOGRAPHIES

Bekir GECER Maltepe, Istanbul, in 2022. He received the B.S. degree in electrical-electronic engineering from the Fatih University, Istanbul, in 2014 and M.S. degree in electrical-electronic engineering from the Marmara University, Istanbul, in 2019. He is a Ph.D. student at Marmara University. He works as a Lecturer at Atasehir Adiguzel MYO for the Machine and Metal Technology Department, Istanbul. His research areas are electric motors, power electronic and control systems.

N. Fusun SERTELLER She received her degree and M.Sc. in electrical engineering, from Istanbul Technical University (ITU), in Istanbul. She received her Ph.D. degree from Marmara University (MU), Technical Education Faculty Electrical Education Department in Istanbul, Turkey in 2000.

She is currently lecturing on magnetic field theory, electric machines, and numerical methods in Electric-Electronic Engineering Department at MU. Her research interests include electric machine modeling, electrical machine design, electric vehicle motors, mathematical modeling of electric machines and systems, and electromagnetic field theory applications.

Hüseyin CALIK Merkez, Giresun, in 2022. He received the B.S. degree in electrical-electronic engineering from the Marmara University, Istanbul, in 2001 and Ph.D. degree in electrical-electronic engineering from the Marmara University, Istanbul, in 2004. He is currently lecturing on magnetic electric machines, and power plant in Electric-Electronic Engineering Department at Giresun University.